Differences in Protein Expression between the U251 and U87 Cell Lines

Hezhen LI[1*], Bingxi LEI[1*], Wei XIANG[1], Hai WANG[1], Wenfeng FENG[1], Yawei LIU[2], Songtao QI[1]

[1]Southern Medical University, Nanfang Hospital, Nanfang Glioma Center, Department of Neurosurgery, Guangzhou, China
[2]Southern Medical University, Nanfang Hospital, Nanfang Neurosurgery Research Institution, Guangzhou, China

*Drs. LI and LEI contributed equally to this work.

ABSTRACT

AIM: The U251 and U87 cell lines are commonly used as experimental models of glioblastoma. However, these cells exhibit significant differences in their proliferation, invasion, and migration. The aim of the present study was to compare the protein expression profiles of the U251 and U87 cell lines in order to provide a molecular basis for the observed phenotypic differences.

MATERIAL and METHODS: Isobaric tags for relative and absolute quantitation (iTRAQ) and gene ontology (GO) analyses were performed to detect differentially expressed proteins and to predict protein functions, respectively.

RESULTS: Two hundred and forty-four proteins were highly expressed, while 263 proteins exhibited lower levels of expression, in the U251 cells compared to the U87 cells. In particular, higher expression levels of the proteins, C10orf58, FLNC, PDLIM1, TPM4, and lower expression levels of MYH10, PSIP1, SYNM, SLC9A3R2, BCAM, were verified by qPCR in the U251 cell line versus the U87 cell line. When a GO analysis was applied to the iTRAQ results, the proteins that were highly expressed in the U251 cells were found to differ in their molecular functions, biological processes, cellular distribution, and cellular pathways associated with them compared with the highly expressed proteins detected in the U87 cells.

CONCLUSION: Differentially expressed proteins between the U251 and U87 cell lines are associated with regulation of nicotinamide nucleotide metabolism, RNA splicing, glycolysis, and purine metabolism pathways. Further studies on these pathways may identify whether these various pathways account for the observed phenotype differences between the U87 and U251 GBM cell lines.

KEYWORDS: Glioblastoma, U87 cell line, U251 cell line, Proteome, Gene ontology

■ INTRODUCTION

Glioblastoma (GBM) is the most frequently diagnosed primary malignant brain tumor in adults. Clinically, GBM is the most aggressive brain malignancy identified to date and it remains incurable despite advances in neurosurgery, alkylating agent based-chemotherapy, and radiation (14,20). Correspondingly, the median survival of GBM patients is approximately 15 months and the five-year survival rate is less than 10% (19).

The U251 and U87 cell lines are the most common cell lines used as experimental models of GBM to date. The American Type Culture Collection supplies both cell lines for research, and the U251 malignant glioma cell line is listed as being derived from a 75-year-old male patient who was affected by a pleomorphic glioma that was identified by Ponten and Macintyre (15). Similarly, the U87 glioma cell line is listed as being derived from a female patient who suffered from a pleomorphic glioma (4). The biological characteristics of these two cell lines have been found to differ, particularly regarding cell proliferation, migration, and invasion. For example, U87 cells have exhibited a greater capacity for migration and invasion (2,17).

Corresponding author: Songtao QI, Yawei LIU

E-mail: qisongtaonfyy@126.com, limpduck@163.com

The molecular backgrounds of the U87 and U251 cell lines have not been extensively investigated as a characterization of the phenotypic differences observed between these two GBM cell lines.

The goal of the present study was to reveal differences at the molecular level between the U87 and U251 cell lines using a proteomics strategy in order to better understand the differences in the biological phenotypes of these two cell lines and to more effectively target GBM for treatment.

■ MATERIAL and METHODS

Cell culture

Human GBM cell lines, U87 and U251, were purchased from the Chinese Academy of Sciences (Shanghai, China) and were grown in Dulbecco's modified Eagle's medium (DMEM; Gibco, Carlsbad, CA, USA) containing 4.5 g/L glucose, 10% fetal bovine serum (FBS; Gibco), 100 U/mL penicillin, and 100 mg/mL streptomycin (Gibco). The cells were maintained at 37°C in a humidified incubator with 5% CO_2.

Cell Proliferation Assays

Cell proliferation rates were determined with a CCK-8 kit (Dojindo, Kumamoto, Japan) according to the manufacturer's instructions.

Wound Scratch Assay

After cells were plated in 6-well culture plates and had achieved a confluent monolayer, a single linear scratch was made through the cells in each well with a 20 ml tip. Cell movement in response to the wounds was imaged 0, 6, 12, 24, and 48 hours after the scratches had been made.

Transwell detection

Cells (1×10^4 cells in 100 ml DMEM medium without FBS) were seeded on polycarbonate membrane inserts in a Transwell apparatus (Costar, Cambridge, MA, USA). In the lower chamber, 500 ml of conditioned medium containing 10% FBS was added as a chemo-attractant. After the cells were incubated for 8 hours at 37 °C in a 5% CO_2 atmosphere, the inserts were removed from the Transwell plates and were washed with PBS. The cells on the top surface of the insert were removed with a cotton swab, while the cells that were adherent to the lower surface were fixed with methanol and were stained with 0.1% crystal violet solution. The number of cells in six high-resolution fields on each lower surface was counted under a microscope. All of these assays were independently repeated at least three times.

Two-dimensional electrophoresis (2-DE)

Extracts of U251 and U87 cells were each collected with RIPA lysis buffer (Sigma, St. Louis, MO, USA) and then were separated with one-dimensional isoelectric focusing (IEF) followed by two-dimensional sodium dodecyl sulfate polyacrylamide gel electrophoresis (SDS-PAGE), according to the manufacturer's instructions (Amersham Biosciences).

Image analysis was performed using the PDQuest system (BioRad), according to the manufacturer's protocol. To account for experimental variations, a three-spot pattern for each gel was prepared for each cell line. Spot detection, quantification (%, volume), and pattern matching were performed by the PDQuest system.

Isobaric tags for relative and absolute quantitation (iTRAQ)

Total protein extracts were collected from U251 and U87 cells with RIPA lysis buffer (Sigma). Following a digestion step with Trypsin Gold (Promega, Madison, WI, USA), the resulting peptides were dried, reconstituted in 0.5 M triethylammonium bicarbonate (TEAB) buffer (Applied Biosystems, Milan, Italy), and then processed with 8-plex iTRAQ reagent (Applied Biosystems), according to the manufacturer's protocol. The samples were labeled with the following iTRAQ tags: U251 (113 and 115) and U87 (114 and 116 tags) as appropriate. Strong cation exchange (SCX) chromatography was performed with a LC-20AB HPLC Pump system (Shimadzu, Kyoto, Japan), then data were acquired with a TripleTOF 5600 System (AB SCIEX, Concord, Ontario, Canada) fitted with a Nanospray III source (AB SCIEX) and a pulled quartz tip as the emitter (New Objectives, Woburn, MA, USA).

Real-Time polymerase chain reaction (PCR)

Total ribonucleic acid (RNA) was extracted from the U251 and U87 cell lines with Trizol reagent (TAKARA, Dalian, China). Levels of Tropomyosin alpha-4 chain (TPM4), Filamin-C (FLNC), Redox-regulatory protein FAM213A (C10orf58), PDZ and LIM domain protein 1 (PDLIM1), Myosin-10 (MYH10), PC4 and SFRS1-interacting protein (PSIP1), Synemin (SYNM), Na(+)/H(+) exchange regulatory cofactor NHE-RF2 (SLC9A3R2), and Basal cell adhesion molecule (BCAM) mRNA were detected with the Quantitect SYBR Green PCR kit (TAKARA) with a ABI 7500 quantitative PCR system (TAKARA), according to the manufacturer's instructions. GAPDH mRNA was used as an internal control for determining the relative amounts of mRNA according to the comparative ΔΔCt method as described previously (8). In addition, fold-change was calculated with the 2-ΔΔCt equation. The primers are listed in Table I.

Bioinformatics analysis

After differentially expressed proteins were detected between the U87 and U251 cell lines with a proteomics method, these data were submitted to the Enrichment analysis (beta) server of the Gene Ontology Consortium (http://geneontology.org/). Briefly, the dataset was analyzed using the Core Analysis module to rank the proteins according to their molecular function, associated biological process, cellular component, and associated pathway(s).

Statistical Analysis

All data are presented as the mean ± standard deviation (SD). Differences between groups were analyzed by one-way analysis of variance, with a p value less than 0.05 considered statistically significant (two-tailed).

Table I: Primers Sequences Used in this Study

Name	F/R	Sequence (5' – 3')
GAPDH*	F	ATCATCAGCAATGCCTCCTG
	R	ATGGACTGTGGTCATGAGTC
TPM4	F	GCAGATGCTGAAGTTGGACA
	R	GTGAGCTCCAGCTTCTCCTG
FLNC	F	TCACCAACTTCAACCGTGAC
	R	GGGAACTGGGACAGGTAGGT
PDLIM1	F	TCAAAGGCTGCACAGACAAC
	R	TATGGATGACGCTTCCCTTC
C10orf58	F	CCCCCTCTATGCAGTGGTAA
	R	CTGATCCCACCACGAAAACT
MYH10	F	AGGGAAGAAGCGTCATGAGA
	R	TCACTGGTTTAGGCGATTCC
PSIP1	F	TGTAAAGCCACCCACAAACA
	R	GTTGCTGCCTGTTGACTTGA
BCAM	F	GCTGTTGCTCGCAGTCCT
	R	GACTTTCCTCGCATCACCTC
SLC9A3R2	F	GCTATGGGTTCAACCTGCAT
	R	AAGCCGCTTGAAGTGTTCAT
SYNM	F	CTGGAGGATGAGAAGGCAAC
	R	TTCTGACGGCATGTTTTCAA

*Primers used for quantitative PCR; **F:** forward; **R:** reverse.*

■ RESULTS

### Proliferation, migration, and invasion of the U251 and U87 cell lines

In CCK8 assays under parallel conditions, the U87 cells were observed to proliferate at a faster rate than the U251 cells. When the two cell lines were evaluated in wound scratch assays, a significantly higher percentage of U87 cells underwent migration compared with the U251 cells (data not shown). Correspondingly, in Transwell chamber assays, the number of invasive U87 cells was greater than the number of invasive U251 cells.

2-DE of the U251 and U87 cell lines

Proteomic analysis with 2-DE was used to assess the histological origins of the U87 and U251 cell lines. In the silver-stained 2-DE gels obtained, a total of 886 ± 23 protein spots and 913 ± 29 protein spots were detected in the U87 and U251 cell extract samples, respectively (Figure 1 A,B). When these data were analyzed by PDQuest software, only ~11% of the protein spots exhibited more than a two-fold increase or decrease in protein expression (Figure 1 A,B). Based on these results, it appears that these two cell lines were derived from the same histological type of cells.

Differentially expressed proteins were identified between the U251 and U87 cell lines by iTRAQ

To further characterize the protein expression profiles for the U87 and U251 cell lines, relative protein abundance was evaluated with a quantitative proteomic analysis method, iTRAQ. A total of 3660 types of proteins were analyzed by iTRAQ, and 507 proteins exhibited at least a two-fold difference in abundance. Of these, 66 and 78 differentially expressed proteins were up-regulated in the U87 and U251 cell lines, respectively (Table II).
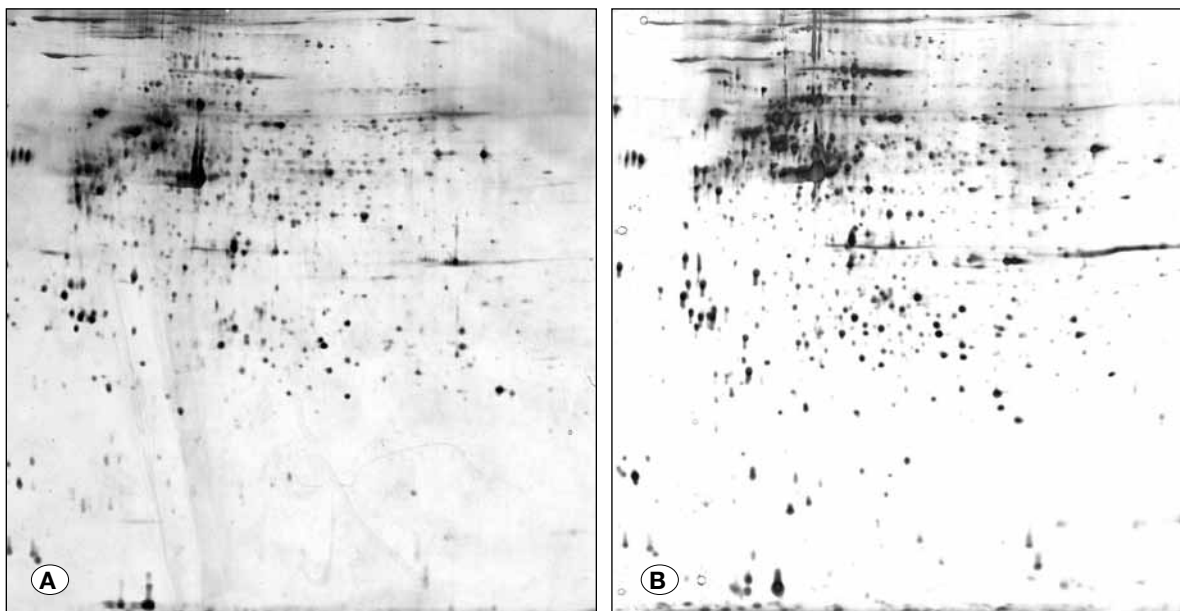
Figure 1: Protein expression profiling that was performed for the extracts collected from the U251 **(A)** and U87 **(B)** cell lines.

Table II: Proteins that are Differentially Expressed Between the U251 and U87 Cell Lines according to the Itraq Analysis Performed

Accession no.	Protein name	Fold-change	Accession no.	Protein name	Fold-change
IPI00218342	C-1-tetrahydrofolate synthase	2.018	IPI00554521	Ferritin heavy chain	2.360
IPI00910114	Isoform 1 of syncoilin	2.245	IPI00010414	PDZ and LIM domain protein 1	7.771
IPI00003818	Kynureninase	3.41	IPI00465431	LGALS3 Galectin-3	2.626
IPI00220301	Peroxiredoxin-6	2.096	IPI00178352	Isoform 1 of Filamin-C	4.918
IPI00007117	Plasminogen activator inhibitor 2	2.236	IPI00005171	HLA-DRA HLA class II histocompatibility antigen	2.843
IPI00924816	Myotrophin	2.262	IPI00031708	Fumarylacetoacetase	3.203
IPI00022229	Apolipoprotein B-100	2.211	IPI00028413	Isoform 1 of Inter-alpha-trypsin inhibitor heavy chain H3	3.976
IPI00296190	C10orf58 UPF0765 protein	4.421	IPI00010491	Ras-related protein Rab-27B	2.603
IPI00102864	Hexokinase-2	2.148	IPI00026663	Aldehyde dehydrogenase family 1 member A3	7.341
IPI00019157	Chondroitin sulfate proteoglycan 4	2.697	IPI00018274	Isoform 1 of Epidermal growth factor receptor	3.757
IPI00020557	Prolow-density lipoprotein receptor-related protein 1	2.017	IPI00219217	LDHB L-lactate dehydrogenase B chain	2.090
IPI00019755	Glutathione S-transferase omega-1	3.217	IPI00916111	Malate dehydrogenase	2.286
IPI00014454	Isoform RIN1 of Ras and Rab interactor 1	3.588	IPI00009943	Tumor protein, translationally-controlled 1	2.823
IPI00027463	Protein S100-A6	2.451	IPI00106668	Perilipin-3 isoform 3	2.107
IPI00168959	Olfactory receptor 1M1	2.295	IPI00009958	Signalosome complex subunit 5	2.309
IPI00216159	Glucosamine fructose-6-phosphate aminotransferase 2	2.496	IPI00478003	Alpha-2-macroglobulin	5.708
IPI00018873	Nicotinamide phosphoribosyltransferase	3.912	IPI00100106	Isoform 3 of Synembryn-A	2.096
IPI00010471	LCP1 Plastin-2	2.535	IPI00304409	Calcium-regulated heat stable protein 1	2.351
IPI00179700	Isoform HMG-1 of high mobility group protein HMG-I/HMG-Y	3.242	IPI00219025	Glutaredoxin-1	2.173
IPI00218733	Superoxide dismutase	2.385	IPI00746777	Alcohol dehydrogenase class-3	2.349
IPI00293276	Macrophage migration inhibitory factor	4.647	IPI00329801	Annexin A5	2.013
IPI00179743	Isoform 1 of sequestosome-1	2.121	IPI00216975	Isoform 2 of Tropomyosin alpha-4 chain	5.037
IPI00017184	EH domain-containing protein 1	2.018	IPI00289758	Calpain-2 catalytic subunit	2.126
IPI00783862	Flavin reductase	2.290	IPI00219344	Hippocalcin-like protein 1	2.312
IPI00007750	Tubulin alpha-4A chain	2.927	IPI00020356	Uncharacterized protein	3.184
IPI00386208	Gastric-associated differentially-expressed protein YA 61P	7.266	IPI00008552	Glutaredoxin-3	2.011
IPI00549343	Vesicle-associated membrane protein 3	2.463	IPI00012007	Adenosylhomocysteinase	2.061
			IPI00216508	Isoform 2 of Sorting nexin-3	2.100
IPI00180128	Basic leucine zipper and W2 domain-containing protein 1	2.264	IPI00217966	Isoform 1 of L-lactate dehydrogenase A chain	8.879
IPI00032426	Isoform 1 of Protein MEMO 1	2.641	IPI00022200	Isoform 1 of Collagen alpha-3(VI) chain	2.661
IPI00027341	Macrophage-capping protein	3.425	IPI00021828	Cystatain-B	4.952
IPI00744692	Transaldolase	2.065	IPI00011726	Isoform 1 of RNA 3-terminal phosphate cyclase	2.009

Table II: Cont.

Accession no.	Protein name	Fold-change
IPI00178440	EEF1B2 Elongation factor 1-beta	2.002
IPI00010402	Putative uncharacterized protein	3.661
IPI00219446	Phosphatidylethanolamine-binding protein 1	2.324
IPI00215948	Isoform 1 of Catenin alpha-1	0.498
IPI00747849	Sodium/potassium-transporting ATPase subunit beta-1	0.458
IPI00021431	COUP transcription factor 1	0.251
IPI00783919	Uncharacterized protein	0.329
IPI00306322	COL4A2 Collagen alpha-2(IV) chain	0.284
IPI00373877	Isoform 1 of Zinc finger protein 326	0.323
IPI00018534	Histone H2B type 1-L	0.381
IPI00013860	3-Hydroxyisobutyrate dehydrogenase	0.435
IPI00299116	Podocalyxin-like isoform 2 precursor	0.420
IPI00386418	Isoform 2 of Myelin expression factor 2	0.378
IPI00376503	Pyrroline-5-carboxylate reductase 1	0.348
IPI00005792	Isoform 1 of Polyadenylate-binding protein 2	0.476
IPI00010348	Deoxyribonuclease-2-alpha	0.472
IPI00171438	Thioredoxin domain-containing protein 5	0.413
IPI00397526	Isoform 1 of Myosin-10	0.235
IPI00010388	Major centromere autoantigen B	0.366
IPI00031713	CD70 antigen	0.422
IPI00217871	Delta-1-pyrroline-5-carboxylate dehydrogenase	0.377
IPI00008986	Large neutral amino acids transporter small subunit 1	0.188
IPI00217975	Lamin-B1	0.330
IPI00216046	SMARCA1 SWI/SNF related, matrix associated, actin dependent	0.441
IPI00019869	Protein S100-A2	0.077
IPI00180404	Isoform 1 of Nexilin	0.351
IPI00297477	U2 small nuclear ribonucleoprotein A~	0.464
IPI00021267	Ephrin type-A receptor 2	0.217

Accession no.	Protein name	Fold-change
IPI00797136	Inhibitor of nuclear factor kappa-B kinase-interacting protein	0.482
IPI00220528	Small nuclear ribonucleoprotein F	0.430
IPI00301936	Highly similar to ELAV-like protein 1	0.438
IPI00028122	Isoform 1 of PC4 and SFRS1-interacting protein	0.255
IPI00021924	Histone H1x	0.300
IPI00550239	Histone H1.0	0.349
IPI00020944	Squalene synthase	0.324
IPI00002406	Basal cell adhesion molecule	0.248
IPI00026272	Histone H2A type 1-B/E	0.433
IPI00020719	Isoform 1 of Mitochondrial antiviral-signaling protein	0.468
IPI00470805	Isoform 2 of Mediator of DNA damage checkpoint protein 1	0.449
IPI00003406	Isoform 1 of Drebrin	0.493
IPI00013159	Transcription factor ETV6	0.273
IPI00220194	Facilitated glucose transporter member 1	0.330
IPI00061178	Heterogeneous nuclear ribonucleoprotein G-like 1	0.451
IPI00641829	Isoform 2 of Spliceosome RNA helicase	0.484
IPI00292771	Isoform 1 of Nuclear mitotic apparatus protein 1	0.457
IPI00217467	Histone H1.4	0.185
IPI00027493	Isoform 2 of 4F2 cell-surface antigen heavy chain	0.446
IPI00385034	Isoform 1 of Na(+)/H(+) exchange regulatory cofactor NHE-RF2	0.187
IPI00299468	Acyl-CoA desaturase	0.361
IPI00018278	Histone H2A.V	0.437
IPI00029081	Isoform Alpha of DNA ligase 3	0.478
IPI00158020	SWAP/Surp domain containing protein	0.457
IPI00554788	Type I cytoskeletal 18	0.155
IPI00470924	Isoform 2 of Transmembrane and TPR repeat-containing protein 3	0.340
IPI00797038	Phosphoenolpyruvate carboxykinase [GTP], mitochondrial	0.387

Table II: Cont.

Accession no.	Protein name	Fold-change
IPI00443799	Putative sodium-coupled neutral amino acid transporter 10	0.389
IPI00016915	Insulin-like growth factor-binding protein 7	0.287
IPI00296099	Thrombospondin-1	0.347
IPI00008570	Isoform 1 of KH domain-containing, RNA-binding	0.442
IPI00015102	Isoform 1 of CD166 antigen	0.206
IPI00045839	Isoform 1 of Prolyl 3-hydroxylase 1	0.442
IPI00023673	Galectin-3-binding protein	0.367
IPI00031131	Isoform 1 of Adipocyte plasma membrane-associated protein	0.293
IPI00152853	Isoform 1 of Phostensin	0.488
IPI00022095	Isoform RF1/RF2 of Retrotransposon-derived protein PEG10	0.340
IPI00337541	NAD(P) transhydrogenase	0.498
IPI00219425	Isoform Beta of Poliovirus receptor	0.304
IPI00221384	Isoform 2 of Collagen alpha-1(XII) chain	0.311

Accession no.	Protein name	Fold-change
IPI00555902	Isoform 1 of OCIA domain-containing protein 2	0.488
IPI00032343	Uncharacterized protein DKFZp762I1415	0.492
IPI00022977	Creatine kinase B-type	0.358
IPI00240812	PDS5B Uncharacterized protein	0.377
IPI00103554	Transcriptional repressor p66-beta	0.448
IPI00395887	Thioredoxin-related transmembrane protein	0.320
IPI00219301	Myristoylated alanine-rich C-kinase substrate	0.247
IPI00299301	Isoform 1 of Synemin	0.250
IPI00006079	Isoform 1 of Bcl-2-associated transcription factor 1	0.377
IPI00168262	Procollagen galactosyltransferase 1	0.435
IPI00005578	EH domain-containing protein 4	0.435
IPI00031008	Isoform 1 of Tenascin	0.371
IPI00291916	PH-interacting protein	0.395

Nine differentially expressed genes were specifically analyzed by qPCR

Quantitative PCR was performed to detect the expression levels of nine proteins that were found to be differentially expressed between the U251 and U87 cell lines by 2-DE. These proteins included: C10orf58, FLNC, PDLIM1, TPM4, MYH10, PSIP1, SYNM, SLC9A3R2, and BCAM. Levels of C10orf58, FLNC, PDLIM1, and TPM4 were higher in the U251 cell extracts than in the U87 cell extracts (Table III). Conversely, the expression levels of MYH10, PSIP1, SYNM, SLC9A3R2, and BCAM were lower in the U251 cell extracts compared with the U87 cell extracts. Both sets of results were consistent with the iTRAQ results obtained.

A bioinformatics analysis of the differentially expressed proteins identified

To identify the possible functions of the proteins separated by identified with iTRAQ, a widely used, web-based analysis tool was employed, Geneontology (GO; http://geneontology.org/) (3). The goal of a GO analysis is to describe a gene product in relation to the biological processes, molecular function, and cellular distribution described according to its previous annotations.

The top ten biological processes that were associated with the highly expressed proteins detected in the U87 cells were: Oxidation-reduction, cellular component organization or biogenesis, cellular component organization, mRNA processing, RNA splicing, macromolecular complex subunit organization, metabolism, metabolism of organic substances, cellular metabolism, and primary metabolism (Figure 2). In the U251 cells, the top ten biological processes were: Small molecule metabolism, carboxylic acid metabolism, nucleobase-containing small molecule metabolism, nicotinamide nucleotide metabolism, pyridine nucleotide metabolism, nucleotide metabolism, nucleoside phosphate metabolism, oxoacid metabolism, oxidoreduction coenzyme metabolism, and pyridine-containing compound metabolism (Figure 2).

The top ten molecular functions that were associated with the highly expressed proteins detected in the U87 cells were: Poly(A) RNA binding, RNA binding, protein binding, binding, organic cyclic compound binding, heterocyclic compound binding, nucleic acid binding, macromolecular complex binding, oxidoreductase activity, and protein complex binding (Figure 3). For the U251 cells, the top ten molecular functions identified were: Protein binding, binding, catalytic activity, small molecule binding, nucleoside phosphate binding, nucleotide

Table III: The Relative Expression of Ten Differentially Expressed Genes that were Identified from Proteomic Profiling of U251 and U87 Cell Lines

Protein	BCAM	PSIP1	SLC9A3R2	MYH10	SYNM	c10orf58	FLNC	PDLIM1	TPM4
Expression ratio* (U87/U251)	0.002	0.182	0.001	0.0007	0	27.3	1105	337.8	286

*$P<0.01$.
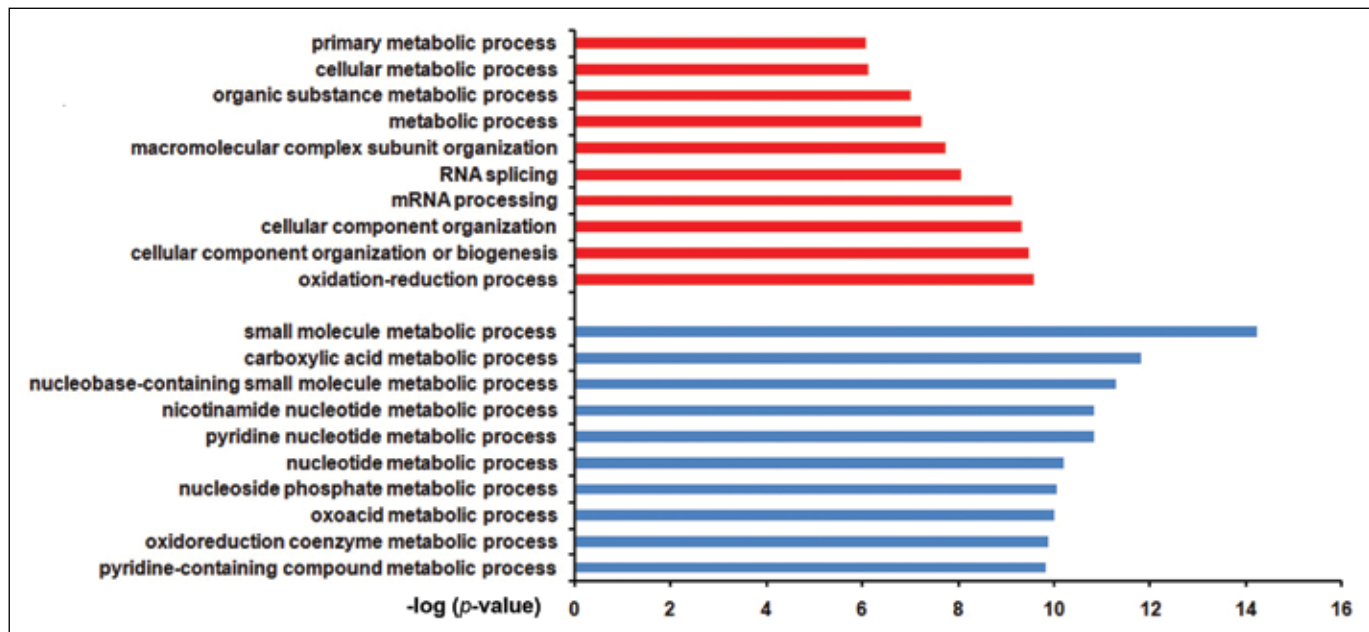
Figure 2: The results of a GO analysis to identify the top 10 biological processes associated with the significantly overexpressed proteins detected in the U87 (red) and U251 (blue) cell lines.
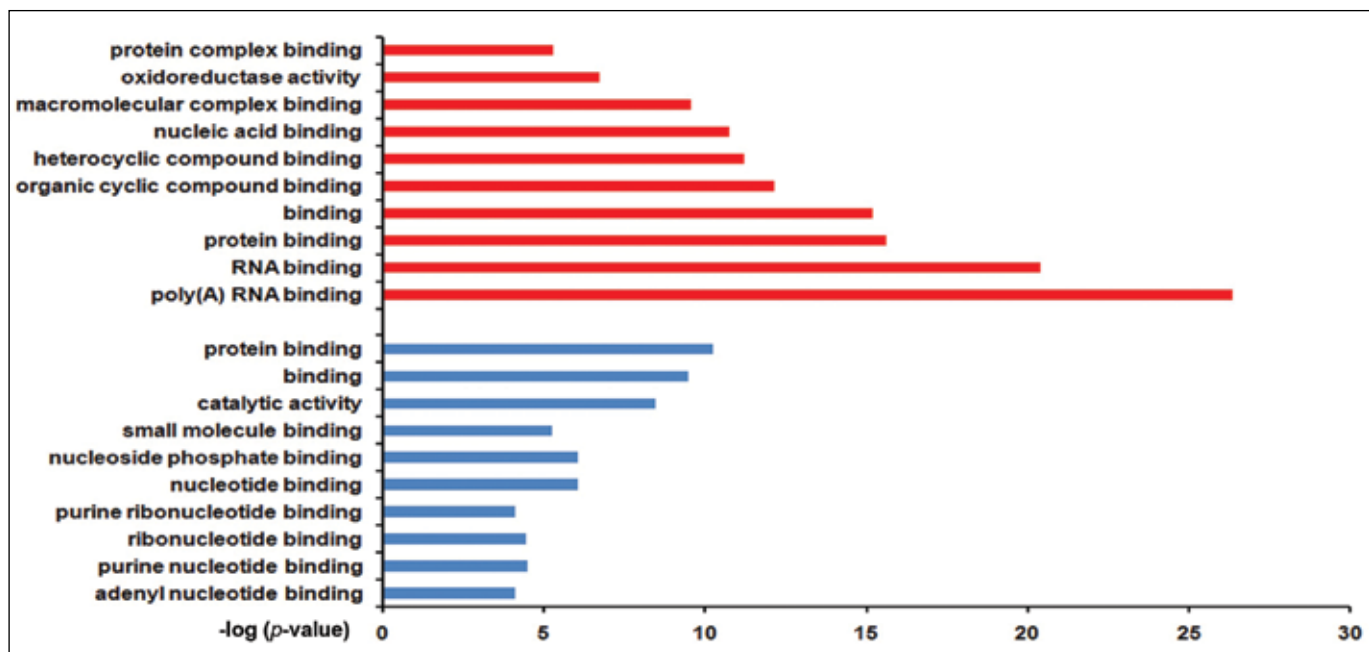
Figure 3: The results of a GO analysis to identify the top 10 molecular functions associated with the significantly overexpressed proteins detected in the U87 (red) and U251 (blue) cell lines.

binding, purine ribonucleotide binding, ribonucleotide binding, purine nucleotide binding, and adenyl nucleotide binding.

The GO analysis also provided results regarding "cellular components", which include descriptions of the distribution/ localization pattern of the proteins identified. For the proteins that were highly expressed in the U87 cells, the top ten cellular distribution annotations were: Intracellular organelle, organelle, membrane-bound organelle, membrane-enclosed lumen, intracellular organelle lumen, organelle lumen, intracellular membrane-bound organelle, intracellular organelle, and intracellular (Figure 4). For the U251 cells, the top ten cellular distribution annotations were: Extracellular exosome, extracellular membrane-bound organelle, extracellular organelle, extracellular vesicle, vesicle, membrane-bound vesicle, cytosol, cytoplasm, extracellular, and cytoplasmic (Figure 4).

PANTHER is a comprehensive, curated database of protein families, trees, subfamilies, and functions (10). As such, it was applied to provide further pathway enrichment analysis of the proteomic data obtained. For the U87 protein data, no significant pathway clusters were found to be associated with the proteins that were highly expressed in the proteomics assays performed. However, for the U251 protein data, six clustered pathways were associated with the highly expressed proteins identified, and these included: Glycolysis, the pentose phosphate pathway, fructose galactose metabolism, *de novo* purine biosynthesis, the ubiquitin proteasome pathway, and N-acetylglucosamine metabolism (Figure 5).

■ **DISCUSSION**

In vitro experiments have previously demonstrated that
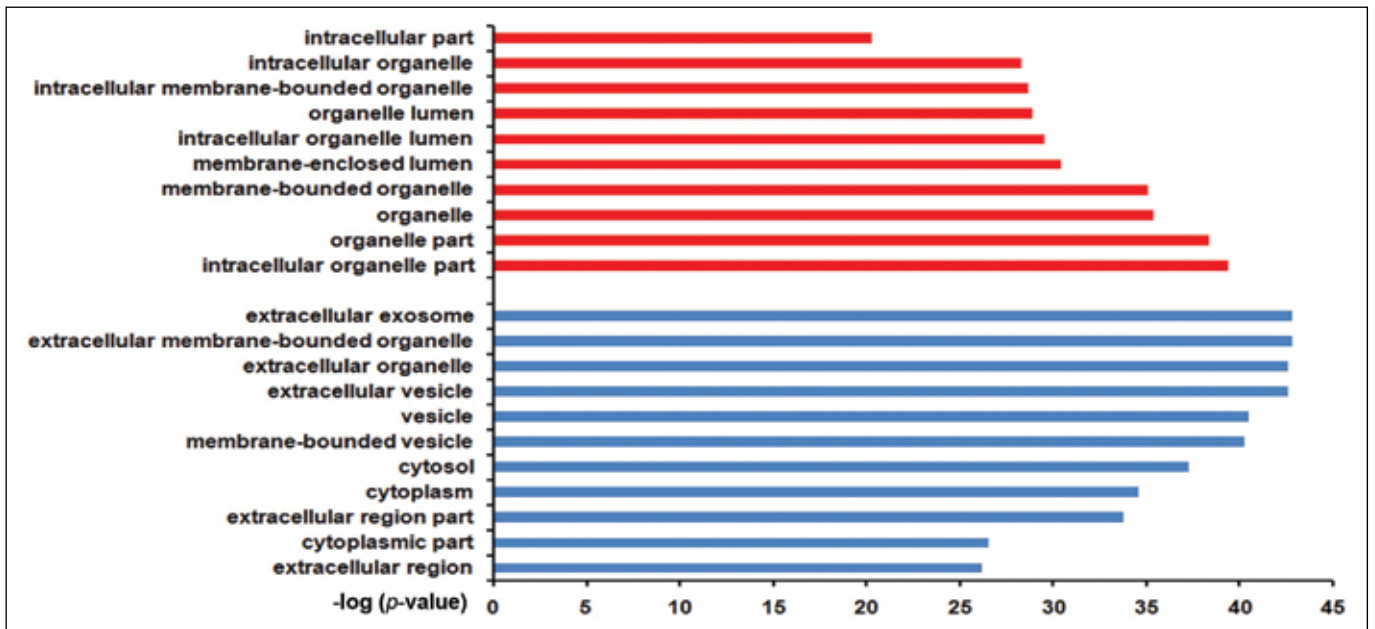
Figure 4: The results of a GO analysis to identify the top 10 cellular distribution annotations associated with the significantly overexpressed proteins detected in the U87 (red) and U251 (blue) cell lines.
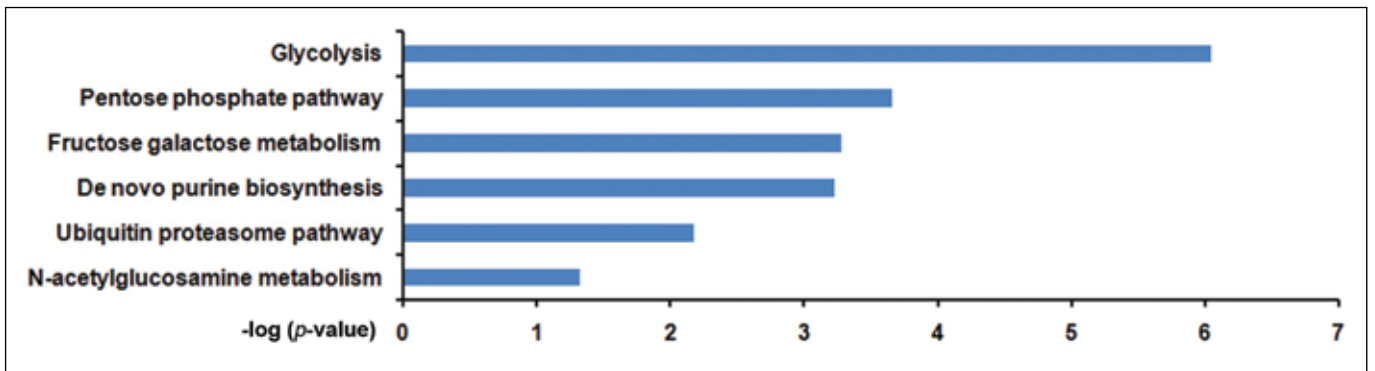
Figure 5: The pathways associated with six of the proteins that were found to be up-regulated proteins in U251 versus U87 cells. The pathway categories are indicated along the vertical axis, while the horizontal axis represents the enrichment of the pathways. A p value < 0.05 was used as the threshold for identifying significantly overexpressed pathways.

phenotypic differences exist between U251 cells and U87 cells (18). Correspondingly, in the present study, the U87 cells proliferated and migrated faster than the U251 cells under the same conditions. To investigate the molecular basis for these differences, a proteomics study was conducted to detect differences in the protein expression profiles between these two GBM cell lines. Following the application of 2-DE and iTRAQ to the cell extract samples and data collected, both the U251 cells and the U87 cells were found to be derived from GBM, and this is consistent with ATCC records. In addition, 507 proteins exhibited greater than a 2-fold difference in abundance between the two cell lines, and the data for nine of these proteins were confirmed in qPCR assays to detect mRNA levels.

A GO analysis was subsequently performed to derive biological functions from the proteomic data obtained. Potential interactions between the clustered GO terms were identified by using OLSVis (http://ols.wordvis.com/). As a result, proteins that were found to be highly expressed in the U251 cells were associated with biological processes related to the metabolism of nicotinamide nucleotides and carboxylic acid, adenyl nucleotide binding was identified as a molecular function, and the cellular distribution most commonly annotated was extracellular. For the proteins highly expressed in the U87 cells, the associated biological processes were focused on mRNA processing and RNA splicing, poly(A) RNA binding was the molecular function identified, and the most common cellular distribution annotated was intracellular. Thus, the biological processes and molecular functions of the two cell lines were found to coincide with the glycolysis and *de novo* purine biosynthesis pathways. Moreover, these results further indicated that the phenotypic differences between the two cell lines may involve the regulation of nicotinamide nucleotide metabolism and RNA splicing. In addition, the primarily extracellular localization of the proteins that were found to be highly expressed in U251 cells may have contributed to the reduced migration capacity that was observed for the U251 cells.

The metabolism pathway for nicotinamide nucleotides involves any nucleotide in combination with nicotinamide, and these substrates are vital for energy transduction and intracellular signaling pathways. Accordingly, nicotinamide represents a critical link between energetic and regulatory processes, and nicotinamide adenine dinucleotide (NAD) may represent a possible therapeutic target for the control of different pathological states, including metabolic disorders and neoplastic transformation (5,13).

The glycolysis pathway was also found to be up-regulated in U251 cells. It has been observed that enhanced glycolysis is a well-known feature of cancer cells, and it is referred to as the "Warburg effect". This effect has also been found to be associated with other cancer cell properties such as adaptation to conditions of hypoxia and low nutrient availability, as well as immortalization, resistance to oxidative stress and apoptotic stimuli, and increased biomass synthesis (11). Based on the results of the present study, it is predicted that U251 cells are more resistant to hypoxia and low glucose

conditions. Moreover, the extent to which cells rely on their glycolysis rate versus their mitochondrial respiration rate is a key factor in determining the possible net contribution of autophagy to metabolism (11). This interpretation is consistent with the lower autophagy level that was observed for U251 cells compared with U87 cells in our previous study (9).

Components of the purine metabolic pathway were also enriched in the list of proteins that were up-regulated in the U251 cells. Initially, the *de novo* synthesis of purine nucleotides creates inosine-5'-monophosphate (IMP). IMP represents a branch point for purine biosynthesis, since it can be converted either to guanosine-5'-monophosphate (GMP) by IMPDH2 or to adenosine-5'-monophosphate. Generally, disruption of purine nucleotide metabolism results in an accumulation and/or a lack of ribonucleotides, deoxyribonucleotides, or metabolic intermediates, and this can have potentially cytotoxic consequences (16). Therefore, based on the present results, it is predicted that drugs that target purine metabolism are more cytotoxic to U251 cells than to U87 cells. Currently, there are several inhibitors of purine metabolism that have been approved for clinical use, and these include methotrexate (which inhibits the *de novo* synthesis of purines via dihydrofolate reductase) (6), ribavirin, mycophenolic acid (an inhibitor of IMPDH2) (1,21), and forodesine (an inhibitor of PNP) (7,12).

■ CONCLUSION

Differences in nicotinamide nucleotide metabolic process regulation, RNA splicing, glycolysis, and purine metabolism exist between the U87 and U251 cell lines. Moreover, these differences may account for the distinct phenotypes of these GBM cell lines, and further studies are needed to confirm these possibilities.

■ ACKNOWLEDGMENTS

■ REFERENCES

1. Allison AC, Eugui EM: The design and development of an immunosuppressive drug, mycophenolate mofetil. Springer Semin Immunopathol 14:353-380, 1993

2. Arif T, Vasilkovsky L, Refaely Y, Konson A, Shoshan-Barmatz V: Silencing VDAC1 expression by siRNA inhibits cancer cell proliferation and tumor growth in vivo. Mol Ther Nucleic Acids 3: 159, 2014

3. Ashburner M, Ball CA, Blake JA, Botstein D, Butler H, Cherry JM, Davis AP, Dolinski K, Dwight SS, Eppig JT, Harris MA, Hill DP, Issel-Tarver L, Kasarskis A, Lewis S, Matese JC, Richardson JE, Ringwald M, Rubin GM, Sherlock G: Gene ontology: Tool for the unification of biology. The Gene Ontology Consortium. Nat Genet 25: 25-29, 2000

4. Beckman G, Beckman L, Ponten J, Westermark B: G-6-PD and PGM phenotypes of 16 continuous human tumor cell lines: Evidence against cross-contamination and contamination by HeLa cells. Hum Hered 21:238-241, 1971

5. Di Stefano G, Manerba M, Vettraino M: NAD metabolism and functions: A common therapeutic target for neoplastic, metabolic and neurodegenerative diseases. Curr Top Med Chem 13:2918-2929, 2013

6. Fairbanks LD, Ruckemann K, Qiu Y, Hawrylowicz CM, Richards DF, Swaminathan R, Kirschbaum B, Simmonds HA: Methotrexate inhibits the first committed step of purine biosynthesis in mitogen-stimulated human T-lymphocytes: A metabolic basis for efficacy in rheumatoid arthritis? Biochem J 342 (Pt 1):143-152, 1999

7. Gandhi V, Kilpatrick JM, Plunkett W, Ayres M, Harman L, Du M, Bantia S, Davisson J, Wierda WG, Faderl S, Kantarjian H, Thomas D: A proof-of-principle pharmacokinetic, pharmacodynamic, and clinical study with purine nucleoside phosphorylase inhibitor immucillin-H (BCX-1777, forodesine). Blood 106:4253-4260, 2005

8. Livak KJ, Schmittgen TD: Analysis of relative gene expression data using real-time quantitative PCR and the 2(-Delta Delta C(T)) Method. Methods 25:402-408, 2001

9. Lu Y, Xiao L, Liu Y, Wang H, Li H, Zhou Q, Pan J, Lei B, Huang A, Qi S: MIR517C inhibits autophagy and the epithelial-to-mesenchymal (-like) transition phenotype in human glioblastoma through KPNA2-dependent disruption of TP53 nuclear translocation. Autophagy 11:2213-2232, 2015

10. Mi H, Muruganujan A, Thomas PD: PANTHER in 2013: Modeling the evolution of gene function, and other gene attributes, in the context of phylogenetic trees. Nucleic Acids Res 41:D377-D386, 2013

11. Mikawa T, LLeonart ME, Takaori-Kondo A, Inagaki N, Yokode M, Kondoh H: Dysregulated glycolysis as an oncogenic event. Cell Mol Life Sci 72:1881-1892, 2015

12. Miles RW, Tyler PC, Furneaux RH, Bagdassarian CK, Schramm VL: One-third-the-sites transition-state inhibitors for purine nucleoside phosphorylase. Biochemistry 37:8615-8621, 1998

13. Mouchiroud L, Houtkooper RH, Auwerx J: NAD(+) metabolism: A therapeutic target for age-related metabolic disease. Crit Rev Biochem Mol Biol 48:397-408, 2013

14. Ohgaki H: Epidemiology of brain tumors. Methods Mol Biol 472:323-342, 2009

15. Ponten J, Macintyre EH: Long term culture of normal and neoplastic human glia. Acta Pathol Microbiol Scand 74:465-486, 1968

16. Pospisilova J, Vit O, Lorkova L, Klanova M, Zivny J, Klener P, Petrak J: Resistance to TRAIL in mantle cell lymphoma cells is associated with the decreased expression of purine metabolism enzymes. Int J Mol Med 31:1273-1279, 2013

17. Shchors K, Persson AI, Rostker F, Tihan T, Lyubynska N, Li N, Swigart LB, Berger MS, Hanahan D, Weiss WA, Evan GI: Using a preclinical mouse model of high-grade astrocytoma to optimize p53 restoration therapy. Proc Natl Acad Sci U S A 110:E1480-E1489, 2013

18. Song Y, Luo Q, Long H, Hu Z, Que T, Zhang X, Li Z, Wang G, Yi L, Liu Z, Fang W, Qi S: Alpha-enolase as a potential cancer prognostic marker promotes cell growth, migration, and invasion in glioma. Mol Cancer 13:65, 2014

19. Stupp R, Hegi ME, Mason WP, van den Bent MJ, Taphoorn MJ, Janzer RC, Ludwin SK, Allgeier A, Fisher B, Belanger K, Hau P, Brandes AA, Gijtenbeek J, Marosi C, Vecht CJ, Mokhtari K, Wesseling P, Villa S, Eisenhauer E, Gorlia T, Weller M, Lacombe D, Cairncross JG, Mirimanoff RO: Effects of radiotherapy with concomitant and adjuvant temozolomide versus radiotherapy alone on survival in glioblastoma in a randomised phase III study: 5-year analysis of the EORTC-NCIC trial. Lancet Oncol 10:459-466, 2009

20. Wen PY, Kesari S: Malignant gliomas in adults. N Engl J Med 359:492-507, 2008

21. Zhou S, Liu R, Baroudy BM, Malcolm BA, Reyes GR: The effect of ribavirin and IMPDH inhibitors on hepatitis C virus subgenomic replicon RNA. Virology 310:333-342, 2003